Structure of Hydrated Microporous Aluminophosphates: Static and Molecular Dynamics Approaches of $AlPO_4$-34 from First Principles Calculations

Guillaume Poulet,[†,‡] Philippe Sautet,*[,†,‡] and Alain Tuel[†]

Institut de Recherches sur la Catalyse, Centre National de la Recherche Scientifique, 2 avenue Albert Einstein, 69626 Villeurbanne Cedex, France, and Laboratoire de Chimie Théorique et des Matériaux Hybrides, Ecole Normale Supérieure de Lyon, 46 allée d'Italie, 69364 Lyon Cedex 07, France

Received: February 26, 2002; In Final Form: June 4, 2002

Ab initio density functional theory (DFT) has been used to study the microporous aluminophosphate $AlPO_4$-34 (**CHA** topology) in the calcined dehydrated and rehydrated forms. DFT calculations allowed us first to reproduce experimental observations obtained by X-ray diffraction, solid-state NMR, and thermal analysis and then to obtain a better understanding from dynamical simulations of the structure modifications occurring during hydration of the calcined material. The method and simulation tools were first calibrated on calcined, never-hydrated $AlPO_4$-34. After complete relaxation, the structure was in excellent agreement with the experimental ones. A static approach of the fully hydrated material (with 12 H_2O per unit cell) did not lead to a unique structure but to various polymorphs, differing essentially by the position of the water molecules. A more realistic molecular dynamic approach confirmed that at room-temperature some of the water molecules show large oscillations in the framework and even diffuse within the pores of the aluminophosphate. A combination of structure resolution by Rietveld refinement and molecular dynamics has been proposed to define an average structure and its structural behavior. From the calculated binding energies, the hydration mechanism takes place in one step without the formation of a stable intermediate phase. A structure for the partially hydrated compound (11 H_2O per unit cell) has been determined on the basis of energetic, geometrical, and experimental arguments.

Introduction

Zeolites are compounds that are now widely used as catalysts in petroleum chemistry, especially for the catalytic cracking. In 1982, Flanigen and co-workers[1] discovered a novel class of crystalline microporous aluminophosphates consisting of tridimensional networks of AlO_4^- and PO_4^+ tetrahedra connected by shared oxygen atoms. Their structures and consequently their properties are similar to zeolites. Microporous aluminophosphates (abbreviated as $AlPO_4$-*n*, *n* referring to a structure type) have now drawn considerable attention due to their potential to act as heterogeneous catalysts and molecular sieves.[2,3] They are generally prepared under mild hydrothermal conditions at specific pH values from gels containing sources of aluminum, phosphorus, and organic molecules acting as structure-directing agents. Various structures with different pore sizes and architectures can be created by changing reagents or experimental conditions such as the gel composition, the crystallization temperature, or the crystallization time.[4,5]

Many materials have been derived from $AlPO_4$-*n* by substitution of several elements for framework cations. Among them, MeAPO materials (Me = Co, Ti, Mn)[6] show interesting catalytic activities in the oxidation of organic molecules thanks to the possibility for the incorporated elements to change their oxidation state reversibly without leaving the microporous framework. The family of silicoaluminophosphates (or SAPO) compounds are also of particular interest for their acidic properties.[7,8]

The channels of as-made aluminophosphates are generally filled with organic molecules, and this prevents water molecules from interacting with the hydrophilic structure. In most cases, the organic molecules can be removed by calcination of the as-made product in air at high temperatures without degradation of the microporous structure. When the calcined compound is contacted with air at room temperature, water molecules penetrate the channels and can modify the coordination of framework aluminum species.[9−14] This change in coordination (generally from 4 to 5 or 6 by addition of one or two water molecules) is often accompanied by a reversible structure deformation. The framework modifications depend not only on the structure of the aluminophosphate but also on its composition, MeAPO and SAPO[6,15,16] materials reacting differently from pure $AlPO_4$ systems.[12−14,17−19] Structural changes occurring upon hydration of aluminophosphate frameworks are not well understood. Nevertheless, their knowledge could have a practical impact because they usually modify the pore size and can have consequences on catalytic or separation properties.

Unfortunately, structural studies of calcined rehydrated $AlPO_4$-*n* materials are scarce. One of the reasons is that the peaks in the X-ray diffraction patterns of rehydrated compounds tend to be broad, so structure analysis using Rietveld refinement technique is difficult.[19,20] Theoretical methods could thus be an alternative to experimental techniques.

Since the 1990s, ab initio computational tools have been used to study $AlPO_4$-*n* materials. Van Beest et al.[21] have performed ab initio calculations on a small cluster (H_4SiO_4) to parametrize an interatomic potential of the Buckingham form. They obtained results on quartz and berlinite structures. A consistent molecular mechanics force field has been developed by De Vos Burchart et al.[22] for aluminophosphate structures such as $AlPO_4$-5, -18, -21, -25, -35, -37, VPI-5, and berlinite. Energetics of Si island formation in SAPO-5 and SAPO-34 molecular sieves has been

* To whom correspondence should be addressed. E-mail: sautet@catalyse.univ-lyon1.fr. Fax: (+33) 4 72 44 53 99.
† Institut de Recherches sur la Catalyse.
‡ Ecole Normale Supérieure de Lyon.

10.1021/jp020533p CCC: $22.00
Published on Web 07/30/2002

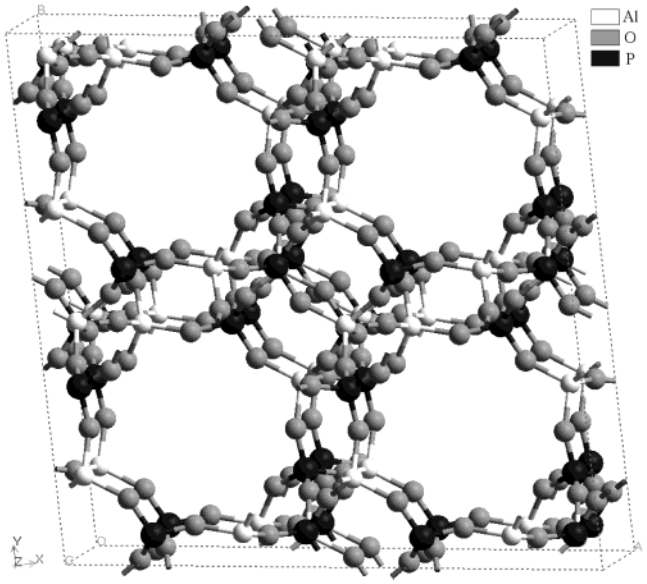

Figure 1. Eight unit cells of the framework structure of dehydrated $AlPO_4$-34 showing the tridimensional open eight-member-ring channel.

studied by Sastre et al.[23] Calculations were performed by interatomic potentials and a shell model was used to simulate the polarizability of the oxygen atoms. Termath et al.[24] have made ab initio simulations (based on density functional theory) of water adsorbed in SAPO-34 with the GGA exchange correlation functional of Perdew and Wang. Raman spectroscopy, thermogravimetry, and NMR along with electronegativity equalization method (EEM)−Monte Carlo calculations have been used by Knops-Gerrits et al.[25] to elucidate the properties of water in Metavariscite, $AlPO_4$-H3, $AlPO_4$-8, and VPI-5.

The aim of the present work is to combine DFT calculations with experimental data to study the structure modifications occurring during hydration of $AlPO_4$-34 (or $AlPO_4$-CHA for chabazite topology[26,27]), for which a reasonably large ensemble of experimental information is known. Figure 1 presents its zeolite-type structure with a tridimensional network of six- and eight- member-rings channels. The structure of this microporous compound remains intact upon calcination, but it distorts dramatically, though in a reversible way, in the presence of water. Following these structural changes by in situ X-ray diffraction (Figure 2) revealed that two stable rehydrated phases, with 12 and 11 water molecules per unit cell, actually exist.[20] Both the dehydrated and fully hydrated structures (with 12 water molecules) are known.[20,28−30] Thus, a direct comparison between experimental and optimized structures for the two types of structures will be possible. Another advantage of this compound is that a large number of test calculations could be performed because of the relatively small number of atoms per unit cell (36 and 72 atoms for the dehydrated and fully hydrated structures, respectively). In this paper, a structural comparison and an energetic study will be presented on the dehydrated and both the fully and incompletely hydrated forms of $AlPO_4$-34.

Computational Methods

The total energy and structure of the various forms of $AlPO_4$-34 defined in the Introduction were determined using the Vienna ab initio simulation program (VASP).[31−35] This code solves the Kohn−Sham equation of density functional theory for periodic systems, developing the one-electron wave function on a basis set of plane wave. The density functional was parametrized in the local-density approximation (LDA), with the exchange-

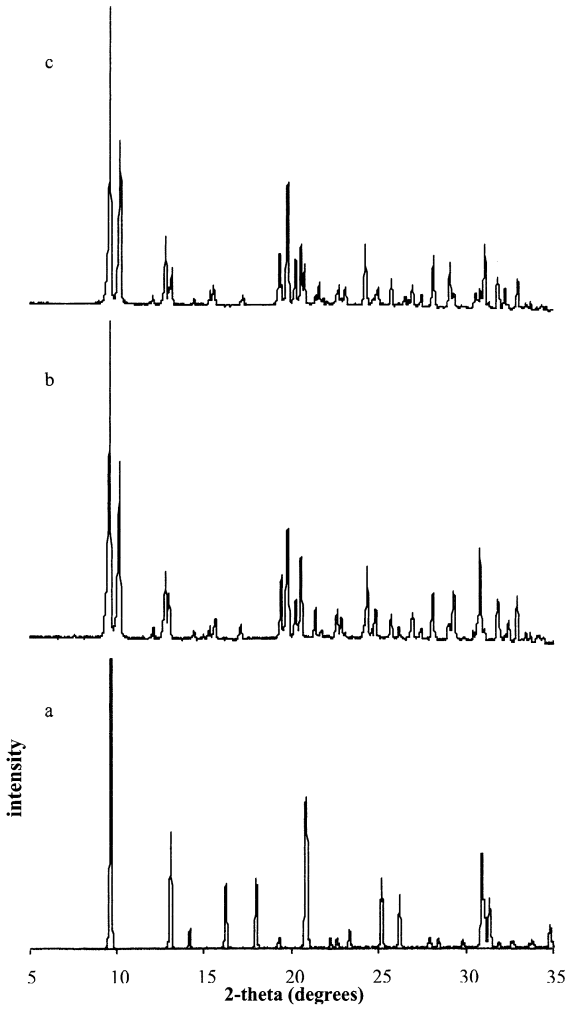

Figure 2. Experimental X-ray powder diffraction patterns of $AlPO_4$-34:[20] (a) calcined (or dehydrated); (b) rehydrated phase **B** (12 H_2O); (c) rehydrated phase **A** (11 H_2O).

correlation functional proposed by Perdew and Zunger[36] and corrected for nonlocality in the generalized gradient approximation (GGA) using the formulation of Perdew and Wang.[37,38] The electron−core interactions were described by ultrasoft pseudopotential,[39,40] which allows us to use a relatively small cutoff of $E_c = 500$ eV for the static approach and 400 eV for the dynamic one. With the highest value (500 eV), the problems related to the incompleteness of the plane wave basis (Pulay stress[41]) are avoided for the static optimization of the crystal cell. The projector-augmented wave method[42,43] has also been recently tested on our dehydrated and hydrated structures. The geometry changes were not significant (less than 1% in cell parameters, less than 0.01 Å in distance and 1° in (Al−O−P) angles). Then, even if we checked all of our results with this more precise approach, our discussion is based here on the results obtained with ultrasoft pseudopotential. Brillouin-zone sampling has been performed with a grid of $1 \times 1 \times 1$ or $2 \times 2 \times 2$ special k points according to the Monkhorst−Pack scheme.[44] We checked that Γ-point calculations are sufficiently precise to obtain converged structures. Two convergence criteria are used. The ionic relaxation is terminated with a change in the total free energy smaller than 10^{-4} eV and atomic forces lower than 0.03 eV $Å^{-1}$. A conjugate-gradient is used to relax the ions into their optimum structure. This code has been already used on zeolite-like compounds similar to $AlPO_4$-n[45−47] and water adsorption on calcium oxide and fluoride surfaces,[48] yielding results in good agreement with experimental data.

As proposed by Jeanvoine et al.,[45] complete structural relaxation was decomposed in several steps. First, the additional hydrogen atoms were relaxed (only for the hydrated structure). Then, a series of relaxations was performed to optimize all of the fractional atomic coordinates, the cell being fixed. Finally, the cell shape and volume were allowed to change, together with all atomic coordinates.

Fixed-volume molecular dynamics runs were conducted in simulated canonical ensemble using the algorithm of Nosé.[49,50] A Verlet velocity algorithm[51] is used to integrate Newton's equations of motion with a time step of 0.5 fs. They were performed at 300 or 400 K for periods ranging from 1 to 3 ps. A maximum temperature of 800 K was used for simulated annealing calculations. Then, the temperature was slowly decreased to 300 K to allow the system to change the hydrogen-bond network and to explore larger regions of the phase space during a trajectory of 2.5 ps.[46]

Hydrogen-bond interactions have a great importance for the structure and stability of $AlPO_4$-*n*. Many experimental and theoretical studies were performed on this interaction.[52−56] The reliability of the considered DFT approach using the PW91 exchange-correlation functional was tested on the water dimer. The geometric and binding energetic results (23.4 kJ mol^{-1}) are in good agreement with experimental values and recent theoretical studies, which validates the selected functional.[57−59]

CaRIne crystallography software[60] was used to simulate X-ray powder diffraction patterns of the different forms of $AlPO_4$-34. The validity of the simulation program was evaluated on the calcined dehydrated and rehydrated $AlPO_4$-34, for which the simulated X-ray powder pattern was compared with the experimental one. No significant differences were observed between the two patterns, thus implying that CaRIne is adapted to the study of our compounds.

Results and Discussion

1. Dehydrated $AlPO_4$-34. The first structure optimizations were performed on calcined dehydrated $AlPO_4$-34. Because the experimental geometry of this aluminophosphate is known from Rietveld refinement of the X-ray powder diffraction pattern, this system was used as a reference for our calculations, principally as a test of the approximations.

The relaxed structure is shown in Appendix 1. Comparison with the experimental structure was made by calculating the atomic displacement between the two structures. The average translation and rotation of the cell was first corrected. To compensate for changes in the unit cell volume, variations (Δx, Δy, Δz) of the crystallographic coordinates were calculated and combined in an atomic displacement using average cell parameters. The calculated values are in excellent agreement with the experimental ones. The largest deviation is 0.06 Å for a group of equivalent oxygen atoms (O_{19-24}).

The simulated X-ray diffraction patterns of experimental and optimized dehydrated $AlPO_4$-34 are given in Figure 3 and a quantitative comparison of respective geometric values is reported in Table 1. The two patterns are perfectly correlated. The only significant difference is that peaks for the calculated structure are slightly displaced toward large angle values. This is explained by a well-known tendency of DFT-GGA to slightly overestimate atomic distances and cell volume. As a result, distances in the reciprocal space are decreased and the diffraction angle increases. As seen from Table 1, the overestimation of bond distances does not exceed 1%. Although no symmetry has been imposed during optimization, only a very little dispersion of the Al−O−P angle and bond lengths (less than 0.01 Å for Al−O and P−O bonds) is observed for the dehydrated structure

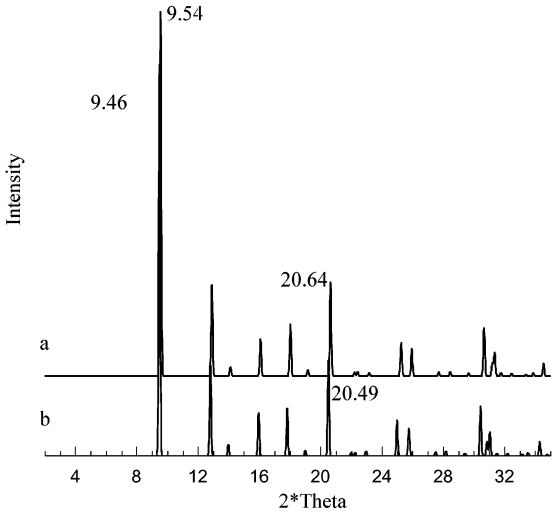

Figure 3. Simulated X-ray powder diffraction patterns of experimental and optimized dehydrated $AlPO_4$-34: (a) simulated X-ray powder diffraction pattern of the optimized with VASP structure; (b) simulated X-ray powder diffraction pattern of the experimental structure (on the basis of coordinates and cell-parameters obtained by Rietveld refinement).

TABLE 1: Quantitative Comparison of Geometric Values between Experimental and Optimized Dehydrated $AlPO_4$-34

unit cell	experimental	optimized with VASP
volume (Å^3)	825.7	833.0
average quadratic difference (Å) (max)		0.033 (0.061)
Al−O distance (Å) (extreme values)	1.739	1.738/1.747
P−O distance (Å) (extreme values)	1.519	1.530/1.539
(Al−O−P) angle (deg) (extreme values)	149.5/150.0	146.5/150.5

(cf. Table 1). Therefore, preliminary results obtained on dehydrated $AlPO_4$-34 are very promising and show that the method can be applied to the more complex hydrated structures.

2. Fully Hydrated $AlPO_4$-34. $AlPO_4$-34 is one of the microporous aluminophosphates for which the structure of the calcined rehydrated material could be determined by Rietveld refinement of the powder diffraction pattern. Actually, all atomic coordinates are known except those of water hydrogen atoms. Consequently, this study will also confirm the ability of DFT calculations to describe structures in which hydrogen-bond interactions play an important role.[45,46,48]

2.1. Optimization of the Structure. The fully hydrated $AlPO_4$-34 contains 12 water molecules per unit cell. Because the positions of hydrogen atoms are not known from X-ray diffraction, 21 different initial structures were randomly generated. First, relaxations were performed from these 21 initial sets, allowing the hydrogen atoms to move. The four relaxed structures with the lowest total energy were then kept, and a full relaxation was thus allowed. The different steps and the corresponding energies are summarized in Table 2, while the lowest energy structure (denoted "$\mathbf{0}_{final}$") is described in Appendix 2. Two different types of water molecules are present in the channels. Six water molecules directly interact with framework Al atoms ($H_2O_{framework}$), while the six remaining ones interact only with other water molecules or framework oxygens by hydrogen bonds ($H_2O_{nonframework}$) (see Figure 4). The framework water molecules are directly connected to the framework by an Al−O bond shorter than 2.5 Å. The corresponding hydrogen atoms form hydrogen bonds with framework oxygens.

Clearly, after complete relaxation (step 2), four structures were found with very similar energies. They differ in the precise connectivity of the hydrogen-bond network. The average atomic

TABLE 2: Energy Evolution of the Best 4 Structures among a Set of 21 Generated with Random Hydrogen Coordinates

	step 1[a]	step 2[b]				step 3[c]		
index of the structure	*E* (eV)	*E* (eV)	unit cell volume (Å^3)	average atomic displacement on 36 framework atoms (Å) (max)	average atomic displacement on the 48 atoms (Å) (max)	*E* (eV)	unit cell volume (Å^3)	
0	−448.145	−448.300	788.0	0.142 (O_{19} = 0.324)	0.224 (O_{46} = 0.882)	−448.547	798.9	→ $\mathbf{0}_{final}$
8	−448.092	−448.289	791.5	0.146 (O_{19} = 0.314)	0.227 (O_{46} = 1.035)	−448.320	798.2	→ $\mathbf{8}_{final}$
11	−448.139	−448.243	780.0	0.148 (O_{26} = 0.369)	0.249 (O_{47} = 0.822)	−448.286	793.5	→ $\mathbf{11}_{final}$
17	−448.071	−448.294	794.5	0.160 (O_{22} = 0.347)	0.230 (O_{46} = 0.763)	−448.327	801.6	→ $\mathbf{17}_{final}$

[a] Complete relaxation of all atoms. [b] Complete relaxation of all atoms and cell parameters. [c] Structures obtained after an initial increase of cell volume by 3% followed by a complete relaxation.

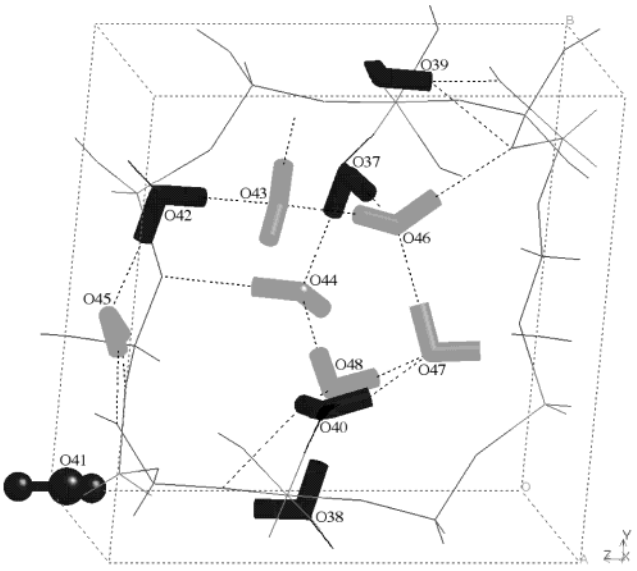

Figure 4. Fully hydrated $AlPO_4$-34 and H-bond network: (dark gray) framework water molecules; (light gray) nonframework water molecules. The water molecule number 41 is drawn in "ball-and-stick". Hydrogen bonds are represented by a dashed line.

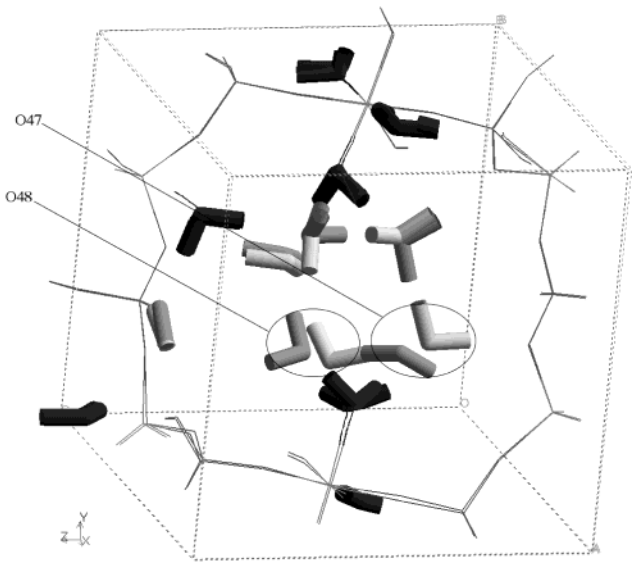

Figure 5. $\mathbf{0}_{final}$ and $\mathbf{8}_{final}$ unit cells superposition.

displacement between each of these four optimized structures and the experimental data are given in Table 2 (step 2). The deviation is small for framework atoms (average 0.16 Å with a maximum of 0.4 Å), whereas very significant displacements are obtained for the oxygen atom of one of the water molecules (up to 1.04 Å). One difficulty of the optimization is that it can lead to metastable structures. Two methods have been used to go beyond these first steps. In the first one, a larger unit cell volume has been imposed, relaxing atomic coordinates, followed by a new complete optimization. The second approach is molecular dynamics to explore the mobility of the various species.

2.1.1. Static Study. In the last step of the optimization, we have imposed an increase in cell volume by 3% for structures **0**, **8**, **11**, and **17**. A larger cell volume decreases the interaction between the water molecules and hence favors potential conformation changes. After optimization, the volume was relaxed. The corresponding energies and unit cell volumes are listed in Table 2, step 3.

The stabilization is significant only for the structure $\mathbf{0}_{final}$, which becomes 250 meV more stable than the others, that is, 21 meV per water molecule. The modifications take place mainly in the position of the hydrogen atoms, that is, the nature of the hydrogen-bond network. Structural changes in structures **8**, **11**, and **17** are negligible. Figure 5 compares the most stable structure $\mathbf{0}_{final}$ with a less stable one, in the present case $\mathbf{8}_{final}$. These two structures show that the largest differences are mainly due to hydrogen atoms of nonframework water molecules (especially O_{47} and O_{48}).

Table 3 compares different structural parameters between the most stable $\mathbf{0}_{final}$ and the experimental structure, while Figure 6 superposes their X-ray powder diffraction patterns. The agreement is not as good as for the dehydrated structure, with a larger average atomic displacement between experimental and theoretical structures (0.28 Å). This is mainly due to the displacement of water molecules. However, in this static approach, even if the various environments of aluminum atoms are correctly described, the framework interatomic distances are somewhat overestimated. For most of the cases, the deviation is lower than 4%, expect for two distances, Al_4-O_{37} and Al_1-O_{31}, which are, respectively, overestimated by 7% and 6% in the calculation. For the Al−O distance between aluminum and coordinated water molecules, the situation is very contrasted. The deviation between experiment and theory is small (2%) for five of the six, while it is very large (13%) for one pentacoordinated aluminum (Al_1-O_{41}). The oxygen atoms of the water molecules are those for which the position is known with the most uncertainty according to the resolution of the structure by Rietveld refinement.[20] A mixture of structures (polymorphism of hydrated aluminophosphates) cannot be excluded. Rotations of the water molecules (keeping oxygen atoms fixed) are indeed not observable by experimental data, and they modify completely the hydrogen-bond network, that is, the energy (cf. Table 2 and Figure 5). The small differences observed between the experimental X-ray powder diffraction pattern and that of the optimized structure $\mathbf{0}_{final}$, principally for $2\theta > 25°$, might be due to the simultaneous presence of different structures in hydrated $AlPO_4$-34. However, the good correlation for angles lower than 25° suggests that these structures are certainly close to $\mathbf{0}_{final}$ (cf. Figure 6a,b).

TABLE 3: Quantitative Comparison of Geometric Values between Experimental, Best Optimized Fully Hydrated $AlPO_4$-34 ($\mathbf{0}_{final}$) and Average Structure from Molecular Dynamics

	Al−O Distance (Å)					
	experimental[a]		optimized with VASP[b]		average structure from molecular dynamics[c]	
	$O_{framework}$	O_{water}	$O_{framework}$	O_{water}	$O_{framework}$	O_{water}
AlO_4[d]	1.700/1.750		1.725/1.778		1.719/1.764	
AlO_5[e]	1.725/1.767	1.99/2.51	1.747/1.888	1.98/2.21	1.747/1.859	1.98/2.54
AlO_6[f]	1.782/1.852	1.99/2.05	1.840/1.927	1.98/2.02	1.812/1.853	1.94/2.04
difference max (%)			7	13	5	3

	P−O Distance (Å)		
	experimental[a]	optimized with VASP[b]	average structure from molecular dynamics[c]
	1.485/1.554	1.498/1.576	1.498/1.566

	Al−O−P Angle (deg)		
	experimental[a]	optimized with VASP[b]	average structure from molecular dynamics[c]
AlO_4[d]	137.2/146.5	133.9/151.8	132.5/152.0
AlO_5[e]	136.8/156.2	125.4/159.4	128.6/156.8
AlO_6[f]	134.5/155.5	142.4/158.9	140.9/158.3

[a] Unit cell volume = 766.5 Å^3. [b] Unit cell volume = 798.9 Å^3. Average atomic displacement for 36 atoms (only framework atoms (6 aluminum, 6 phosphorus and 24 oxygen atoms) = 0.156 (max (O_{32}) = 0.356). Average atomic displacement for 48 atoms (36 framework atoms + 12 oxygen atoms of water molecules) = 0.283 (max (O_{47}) = 1.527). [c] Unit cell volume = 788.0 Å^3. Average atomic displacement for 36 atoms (only framework atoms (6 aluminum, 6 phosphorus and 24 oxygen atoms) = 0.155 (max (O_{22}) = 0.358). Average atomic displacement for 48 atoms (36 framework atoms + 12 oxygen atoms of water molecules) = 0.525 (max (O_{44}) = 3.462). [d] Four-coordinated Al atom (four framework oxygens). [e] Five-coordinated Al atom (four framework oxygens and one water molecule). [f] Six-coordinated Al atom (four framework oxygens and two water molecules).

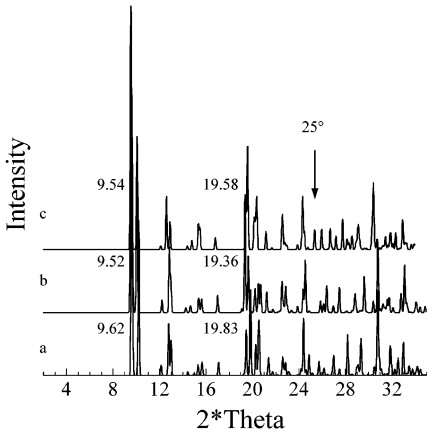

Figure 6. Simulated X-ray powder diffraction patterns of experimental and optimized fully hydrated $AlPO_4$-34: (a) simulated X-ray powder diffraction pattern of the experimental structure (on the basis of coordinates and cell-parameters obtained by Rietveld refinement); (b) simulated X-ray powder diffraction pattern of the optimized with VASP structure ($\mathbf{0}_{final}$); (c) simulated X-ray powder diffraction pattern of a mixture of 40 structures extracted from molecular dynamics (from 0.5 to 2.5 ps).

One important remark concerning the hydrated structures is that the experimental and optimized unit cells contract upon hydration of the calcined structure (from 825.7 to 766.5 Å^3 and from 833.0 to 798.9 Å^3, for the experimental and optimized cells, respectively). The set of water molecules forms a network of strong hydrogen bonds responsible for this reduction of the volume. The water molecules are also responsible for the lower symmetry as compared to the dehydrated cell (change from *R*3*r* to *P*1 symmetry group).

2.1.2. Ab Initio Molecular Dynamics Study. To better understand the polymorphism of hydrated structures, it is important to estimate the mobility of some of the water molecules. Molecular dynamical displacements can be suggested from the values of isotropic displacement parameters (published by Tuel et al.[20]), which convey the idea of large oscillations of framework or nonframework water molecules. This was studied with an ab initio molecular dynamics approach.

A simulated annealing procedure can be used to explore in a more exhaustive way the polymorphic configurations of the hydrated aluminophosphate. The structure was heated to 800 K for 0.2 ps and then cooled to 300 K for a total trajectory of 2.5 ps. After thermalization at 300 K, three types of characteristic behaviors can be underlined for the water molecules: some show just small oscillation around an equilibrium position (such as framework $(H_2O)_{40}$ in Figure 7), others present oscillation with large amplitude (>1 Å for $(H_2O)_{41}$), while some molecules diffuse in the channel with displacement up to 3.2 Å in 2.5 ps.

These results give insight into the mobility of water molecules in the micropores of the aluminophosphate. Framework water molecules have a fixed position, with eventually large potential oscillation amplitudes, whereas nonframework molecules do not show a completely crystalline state with possible diffusion displacements.

An average structure could be obtained from the previous simulated annealing results considering all of the geometries (5000 steps) after thermalization at 300 K. A simulated X-ray powder diffraction pattern was then calculated for the average structure (Figure 6c). Despite the significant oscillations of framework water molecules and the diffusion of some nonframework water molecules, the simulated X-ray powder pattern is not significantly modified as compared to the case of the unique most stable $\mathbf{0}_{final}$ configuration (Figure 6a). Indeed, the diffraction pattern is dominated by atoms of the AlPO framework, for which displacements are negligible as compared to those of water molecule. The agreement between experimental and simulated patterns is not perfect. One of the reasons is that molecular dynamics are performed with constant cell parameters and that these cell parameters are slightly different from the experimental ones. As a consequence, the X-ray diffraction pattern of the calculated average structure is slightly shifted with respect to the experimental pattern.

The static optimized structure and the one averaged along the molecular dynamics can be compared in more details from Table 3, in relation with the experimental data. The average atomic displacements between experiment and theory for the 36 AlPO framework atoms are very similar, but they strongly differ when oxygen atoms of water molecules are considered. The difference can be attributed to large oscillation and even diffusion of these molecules in the channels (Figure 7). In terms of interatomic distances, the quantum molecular dynamics approach

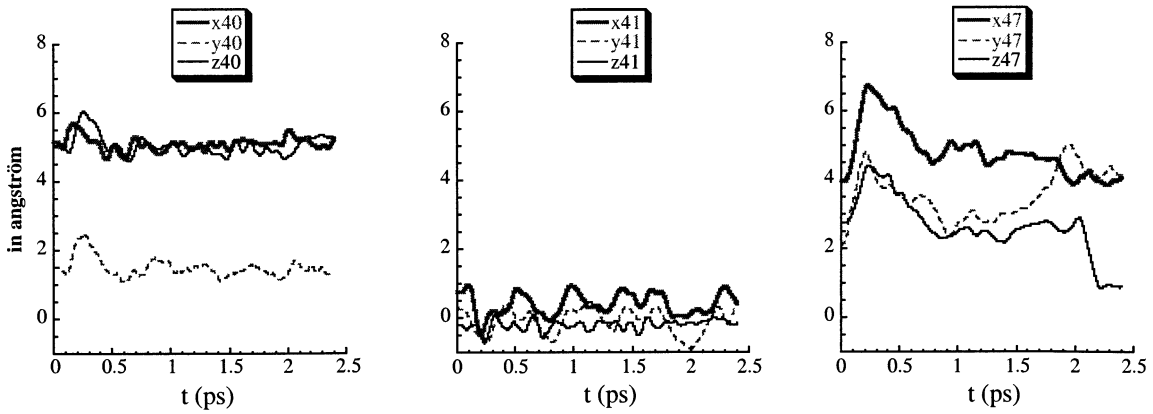

Figure 7. Evolution of atomic Cartesian coordinates of O_{40}, O_{41} (framework water molecules), and O_{47} atoms (nonframework water molecule) in a simulated annealing simulation (final temperature of 300 K).

gives however an improved description in relation with experiments. This is especially the case for Al_1-O_{41} distance, for which the difference switches from 13% in the static approach to 3% in the average dynamic structure. Among framework water molecules, only O_{41} atom moves with an amplitude close to 1 Å at 300 K (Figure 7). Its position is in fact particular. Contrary to the other water molecules, which are all in the eight-membered ring of the chabazite structure, it is located within a double six-ring (D6R) of the framework (cf. the representation of this cage in Figure 8a). This molecule is positioned off center of the D6R unit so that it avoids close contact with P and O atoms. Nevertheless, it can be regarded as "quasi"-coordinated to Al_1. The Al_1-O_{41} distance obtained by Rietveld refinement is 2.51(4) Å, whereas the static optimized Al_1-O_{41} distance in $\mathbf{0}_{final}$ is 2.21 Å (cf. Tables 3 and 4). Figure 8b shows the evolution of the distance and a comparison with other framework molecules such as those corresponding to O_{40} or O_{42}. The Al_1-O_{41} distance oscillates between 2 and 3.3 Å (after 0.5 ps for thermalization), with an arithmetic average of ca. 2.56 Å, very close to that obtained by refinement of the X-ray powder pattern. So, a dynamic description of this weak bond is necessary to define the average position of the molecule as seen by X-ray diffraction. Moreover, it can be noticed that these oscillations are very asymmetric around the static value of 2.21 Å (considered as the equilibrium value). The interaction potential is strongly enharmonic due to a cooperative effect of the other aluminum atoms of the D6R unit, which creates stabilizing interactions when the $(H_2O)_{41}$ molecule moves away from Al_1. This large change in a $Al-(OH_2)$ distance induces some related structural modifications of the Al−O framework distances. As a result, the dynamics of the water molecules have some indirect influence on the structure of the AlPO itself. The two Al−O bonds that showed the largest deviations in the static approach are significantly improved, from 7% to 5% overestimation for Al_4-O_{17} and from 6% to 4% for Al_1-O_{31}. The reduction of Al_1-O_{31} distance is clearly correlated with the increased $Al_1-(OH_2)_{41}$ bond, from a bond order conservation principle around the Al_1 atom. The relation is more indirect for the Al_4-O_{17} bond.

The dynamic approach allows us to describe the vibration, translation, and rotation of water molecule and, consequently, of the hydrogen-bond network. The average displacement of each atom of the hydrated compound, $\langle r^2\rangle^{1/2}$, has been estimated over a set of 10 000 structures (i.e., a 5 ps equivalent trajectory). The average values of $\langle r^2\rangle^{1/2}$ are 0.138, 0.122, 0.204, 0.353, and 0.6 Å for aluminum, phosphorus, framework oxygen, framework water oxygen, and extraframework water oxygen atoms, respectively. Again, these values reflect the high mobility of water molecules, principally those which do not interact directly with the framework, as compared to other atoms such as Al or P. These average displacements can be compared with the square root of isotropic displacements obtained from structure refinement: 0.20, 0.18, 0.19, 0.37, and 0.40 Å for the same type of atoms, respectively. Even though the latter contain additional contributions such as structural defects, they are of the same order of magnitude and follow the same evolution as average displacements calculated from our dynamic study.

Thus, molecular dynamics complete X-ray diffraction for the description of the mobility and statistical positions of atoms, particularly in the case of the O_{41}/Al_1 interaction. Such a synergy between theoretical and experimental tools has already been proposed by Kaszkur et al.[61] to study the positions of heavy atoms (Br) of sorbate molecules within the pore system of zeolite Y.

2.2. Hydration Mechanism. Beyond the structure of the water molecules in the channels, it is important to understand the mechanism of hydration. By comparing the fully hydrated and dehydrated structures, it is possible to evaluate the binding energy per H_2O molecule. This estimation was performed on the most stable $\mathbf{0}_{final}$ configuration. For the fully hydrated structure, an average value of 53 kJ mol^{-1} is found. However, the contribution of framework and nonframework water molecules to this binding energy is not well-defined.

For this purpose, a hypothetical structure containing only the six framework water molecules connected to framework aluminum atoms was considered. Such a "half-hydrated" phase could eventually be considered as an intermediate in the hydration process. For this structure, the binding energy per water molecule is 30 kJ mol^{-1}, that is to say, lower than that for the fully hydrated structure. From this value, the contribution of the nonframework water molecules in the binding energy of the fully hydrated framework can be estimated to 77 kJ mol^{-1}. This energy includes the interaction with the oxygen atoms of the network but also the hydrogen bond with all other water molecules (a total of three or four hydrogen bonds per nonframework water molecule). Hence, these nonframework water molecules, which establish the hydrogen-bond network along the channel, have a key importance in the stability of the structure, while the interaction between aluminum and the bound molecules is only a weak anchoring point. As a consequence, the "half-hydrated" structure cannot be a stable intermediate structure, because a mixture of fully hydrated and dehydrated structures would be more stable. This was confirmed experimentally by following the hydration of calcined $AlPO_4$-34 as a function of time by solid-state NMR and X-ray diffraction. Spectra consisted of a mixture of hydrated and dehydrated forms of $AlPO_4$-34, without any evidence of the presence of a weakly hydrated phase.

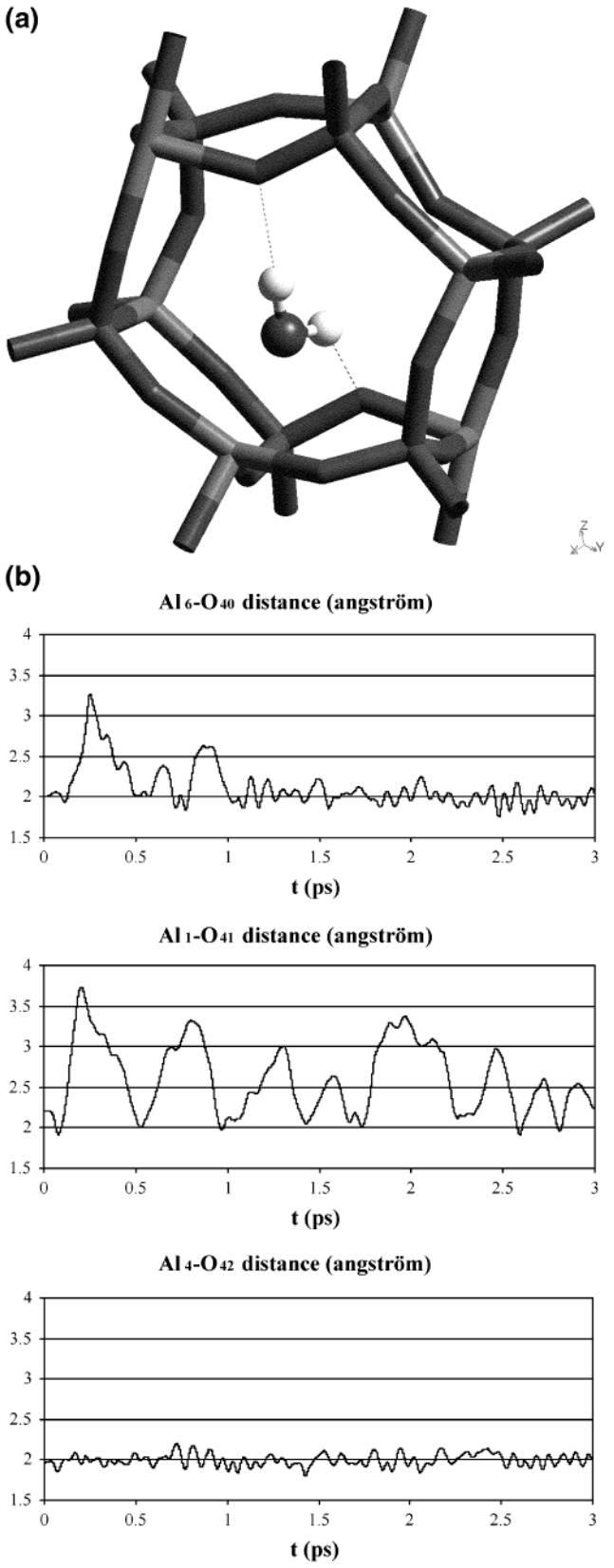

Figure 8. Six-member ring (a) containing the framework molecule O_{41} (in "ball-and-stick") with H-bonds; (b) evolution of Al−O distances during molecular dynamics described in section 2.1.2.

3. Partially Hydrated Phase. Until now, besides the previous half-hydrated model, only the completely hydrated structure with 12 water molecules in the unit cell has been considered. A characteristic of $AlPO_4$-34 is the existence of a second hydrated phase, denoted **A**, containing only 11 water molecules per unit cell and stable between ca. 35 and 55 °C.[20] The thermogravimetric curve shows three consecutive stages corresponding to the three different structures: $T < 35$ °C, phase **B** or fully hydrated $AlPO_4$-34 (12 H_2O); $35 < T < 55$ °C, phase **A** or partially hydrated $AlPO_4$-34 (11 H_2O); $T > 55$ °C, dehydrated phase.

TABLE 4: Energetic and Structural Comparison of the Twelve Different Partially Hydrated Structures (with 11 water molecules instead of 12)

oxygen atom of expelled water molecule	E (eV)	shortest H-bond (number in $\mathbf{0}_{final}$) (<2.5 Å)	Al−O bond in $\mathbf{0}_{final}$ (Å)	average atomic displacement (Å) with $\mathbf{0}_{final}$ (max)[a]
O_{37}	−432.544	1.68 (2)	1.98 (Al3)	0.080 (O_{44} = 0.32)
O_{38}	−432.558	1.65 (3)	1.98 (Al3)	0.092 (O_{48} = 0.37)
O_{39}	−432.716	1.67 (2)	1.99 (Al6)	0.080 (O_{40} = 0.26)
O_{40}	−432.668	1.88 (3)	2.02 (Al6)	0.071 (Al_6 = 0.26)
O_{41}	**−433.222**	**2.03 (2)**	**2.21 (Al1)**	**0.080 (O_{19} = 0.44)**
O_{42}	−432.832	1.73 (2)	1.98 (Al4)	0.161 (O_{26} = 0.45)
O_{43}	−432.810	1.78 (4)		0.038 (O_{46} = 0.25)
O_{44}	−432.740	1.83 (3)		0.037 (O_{48} = 0.18)
O_{45}	−432.779	1.73 (4)		0.035 (O_{42} = 0.13)
O_{46}	−432.647	1.68 (4)		0.052 (O_{47} = 0.36)
O_{47}	−432.700	1.70 (4)		0.038 (O_{46} = 0.21)
O_{48}	−432.657	1.65 (4)		0.046 (O_{44} = 0.19)

[a] Calculated on 47 atoms: 36 framework atoms + 12 oxygen atoms of water molecules − 1 oxygen atom of removed water molecule.

All phase transitions are fast and completely reversible. By contrast to phase **B**, the partially hydrated phase does not exist within a broad temperature range, and a Rietveld refinement of the X-ray powder pattern was not possible. Only the space group and unit cell parameters could be obtained experimentally.[20] These parameters are very similar to those of the fully hydrated phase **B**, and this suggests that both structures are closely related. In particular, we can assume that the position of framework atoms does not significantly change during the phase transition and that the major modifications result from a rearrangement of the water-molecule network inside the channels. Thus, the structure of the fully hydrated $AlPO_4$-34 was used as a starting model for the optimization of the partially hydrated compound.

Each of the 12 water molecules of the unit cell was successively removed and the structure was reoptimized with 11 H_2O. When one of the 12 water molecules is removed, the relaxation of the structure slightly modifies the hydrogen-bond network and the positions of framework atoms. The major modifications are observed for the atoms directly connected or hydrogen-bound to the expelled molecule. However, these modifications remain small, as evidenced by the values of the average atomic displacement between the fully hydrated and the partially hydrated structures (Table 4).

Experimentally, the ^{27}Al MAS NMR spectrum of the hydrated form of $AlPO_4$-34 does not significantly change with temperature between 10 and 50 °C, indicating that the coordination of aluminum atoms and the number of strongly bound framework water molecules are not modified. This suggests that the water molecule responsible for the reversible phase transition is either a nonframework water molecule or a "quasi-framework" molecule, such as that corresponding to O_{41}. The Al_1-O_{41} distance is unusually long for a coordinated water molecule, and the corresponding aluminum atom is seen as tetrahedrally coordinated by solid-state NMR. Therefore, expelling this water molecule from the framework will not modify the NMR spectrum, in particular, the relative proportion of 4-, 5- and 6-coordinate species.

Table 4 lists the energy of the 12 different structures obtained after removal of one of the water molecules. The number of

hydrogen bonds in the initial structure and the shortest distance for these interactions are also given for each molecule. From an energetic point of view, the water molecule corresponding to O_{41} is the best candidate. Moreover, the geometric analysis shows that this molecule is less-involved in the hydrogen-bond network. As already mentioned, this is in agreement with experimental observations: this water molecule does not effectively coordinate an aluminum atom and the NMR spectrum looks similar before and after the phase transition. Furthermore, the reorganization around the missing molecule is not significant. Thus, when the water molecule located in the D6R unit is expelled, the hydrogen-bond network within the chabazite cage is not drastically modified and it remains similar to that of the fully hydrated structure. By contrast, when a water molecule is removed from the channels, its position remains unoccupied in the optimized structure and the energy of the corresponding material is higher. As previously discussed, the network of water molecules located in the channels stabilizes the structure. The water molecule corresponding to O_{41} is the only molecule that can be removed without perturbing the stabilizing effect of the hydrogen-bond network.

Conclusion

The DFT study of structural changes in $AlPO_4$-34 microporous aluminophosphate upon hydration gave results in good agreement with experimental data for both the calcined dehydrated and rehydrated phases. The knowledge of the dehydrated and fully hydrated structures allowed us to calibrate precisely the approach for further studies on this type of compound.

In the case of hydrated structures, crucial insights on the mobility of H_2O molecules at room temperature can be obtained by quantum molecular dynamics. Calculated root-mean-square displacements are in reasonable agreement with the experimental values, and this allowed us to propose a dynamic interpretation of experimental temperature factor issued from Rietveld refinement. In the case of the framework water molecule $(H_2O)_{41}$ showing large displacement amplitudes, the Al−O distance obtained from an average along the trajectory is in much better agreement with the X-ray result than the optimum structure from the static calculation. Thus, intermolecular and even, indirectly, framework interatomic distances are better described by the molecular dynamics approach.

The energy analysis shows that the stability of the hydrated structure is not created by the individual interaction of water molecules with the $AlPO_4$ channel but is ensured by the formation of a collective hydrogen-bond network. This explains why the system shows an abrupt transition between an empty and a full phase with 12 water molecules per unit cell. An additional "quasi-full" phase with 11 molecules observed by X-ray diffraction and thermogravimetric analysis can be associated, from the calculation, with a reversible desorption of the framework water molecule positioned in the double six-ring region of the structure. Removal of this weakly bound molecule has only a moderate effect on the collective hydrogen network. A theoretical structure for this partially hydrated phase has been proposed, in agreement with a large range of experimental results. The quantum chemistry approach developed in the present work appears to be a powerful tool to complete NMR, IR, and X-ray diffraction spectroscopies in the understanding of the hydration process of microporous aluminophosphates.

Information on the polymorphism, that is, the existence of structures with close energies and differing only by the positions of extraframework water molecules, cannot be obtained by X-ray diffraction. Clearly, the resolution of the structure by refinement of the powder pattern provides an average position for the water molecule, even when the latter possesses a significant mobility. Hence, it is suggested that X-ray diffraction techniques should be associated with molecular dynamic approaches to extract more accurate information from experimental and theoretical data. It is obvious that the transferability of such methods to other aluminophosphates will be of practical importance, particularly in the case in which hydrated structures are still unknown.

Acknowledgment. We thank S. Caldarelli and G. Bergeret for their assistance in the interpretation of NMR and diffraction X-ray patterns and M. Digne for numerous and enriching discussions. We acknowledge IDRIS at CNRS for the attribution of CPU time under Project 609.

Appendix 1

Atomic coordinates and structure parameters of experimental and calculated structures for dehydrated $AlPO_4$-34 are shown in Table A1.

TABLE A1: Atomic Coordinates and Structure Parameters of Experimental and Calculated Structures for Dehydrated $AlPO_4$-34[a]

Parameters			
Tuel et al.[20]		calculated	
$a = b = c$	$\alpha = \beta = \gamma$	$a = b = c$	$\alpha = \beta = \gamma$
9.414	94.61	9.442	94.65

Positions							
	Tuel et al.[20]			calculated			atomic displacement
	x	y	z	x	y	z	(Å)
Al1	0.0987	0.3312	0.8778	0.1005	0.3333	0.8771	0.0264
Al2	0.8778	0.0987	0.3312	0.8771	0.1005	0.3333	0.0264
Al3	0.3312	0.8778	0.0987	0.3333	0.8771	0.1005	0.0264
Al4	0.9013	0.6688	0.1222	0.8995	0.6667	0.1229	0.0264
Al5	0.1222	0.9013	0.6688	0.1229	0.8995	0.6667	0.0264
Al6	0.6688	0.1222	0.9013	0.6667	0.1229	0.8995	0.0264
P7	0.3327	0.1110	0.8797	0.3335	0.1112	0.8787	0.0134
P8	0.8797	0.3327	0.1110	0.8787	0.3335	0.1112	0.0134
P9	0.1110	0.8797	0.3327	0.1112	0.8787	0.3335	0.0134
P10	0.6673	0.8890	0.1203	0.6665	0.8889	0.1213	0.0134
P11	0.1203	0.6673	0.8890	0.1213	0.6665	0.8889	0.0134
P12	0.8890	0.1203	0.6673	0.8889	0.1213	0.6665	0.0134
O13	0.2491	0.7339	0.9862	0.2515	0.7336	0.9868	0.0231
O14	0.9862	0.2491	0.7339	0.9868	0.2515	0.7336	0.0231
O15	0.7339	0.9862	0.2491	0.7336	0.9868	0.2515	0.0231
O16	0.7509	0.2662	0.0138	0.7485	0.2664	0.0132	0.0231
O17	0.0138	0.7509	0.2662	0.0132	0.7485	0.2664	0.0231
O18	0.2662	0.0138	0.7509	0.2664	0.0132	0.7485	0.0231
O19	0.1489	0.8619	0.4898	0.1528	0.8570	0.4898	0.0609
O20	0.4898	0.1489	0.8619	0.4898	0.1528	0.8570	0.0609
O21	0.8619	0.4898	0.1489	0.8570	0.4898	0.1528	0.0609
O22	0.8511	0.1381	0.5102	0.8472	0.1430	0.5103	0.0609
O23	0.5102	0.8511	0.1381	0.5103	0.8472	0.1430	0.0609
O24	0.1381	0.5102	0.8511	0.1430	0.5103	0.8472	0.0609
O25	0.2566	0.2472	0.8910	0.2558	0.2468	0.8942	0.0316
O26	0.8910	0.2566	0.2472	0.8942	0.2558	0.2468	0.0316
O27	0.2472	0.8910	0.2566	0.2468	0.8942	0.2558	0.0316
O28	0.7434	0.7528	0.1090	0.7442	0.7532	0.1059	0.0316
O29	0.1090	0.7434	0.7528	0.1059	0.7442	0.7532	0.0316
O30	0.7528	0.1090	0.7434	0.7532	0.1059	0.7442	0.0316
O31	0.0349	0.0149	0.3187	0.0340	0.0154	0.3234	0.0458
O32	0.3187	0.0349	0.0149	0.3234	0.0340	0.0154	0.0458
O33	0.0149	0.3187	0.0349	0.0154	0.3234	0.0340	0.0458
O34	0.9651	0.9851	0.6813	0.9661	0.9846	0.6766	0.0458
O35	0.6813	0.9651	0.9851	0.6766	0.9661	0.9846	0.0458
O36	0.9851	0.6813	0.9651	0.9846	0.6766	0.9661	0.0458

[a] Space group $R3r$ (no. 148). Symmetry operators: (1) x, y, z; $-x, -y, -z$; (2) z, x, y; $-z, -x, -y$; (3) y, z, x; $-y, -z, -x$.

Appendix 2

Atomic coordinates and structure parameters of experimental and calculated structures for fully hydrated $AlPO_4$-34 are shown in Table A2.

TABLE A2: Atomic Coordinates and Structure Parameters of Experimental and Calculated Structures for Fully Hydrated $AlPO_4$-34[a]

Parameters

structures	*a*	*b*	*c*	α	*β*	*γ*
Tuel et al.[20]	9.0259	9.3378	9.5083	95.077	104.08	96.590
$\mathbf{0}_{final}$	9.1851	9.4640	9.5281	94.511	102.89	95.751
$\mathbf{8}_{final}$	9.1385	9.3793	9.4301	94.586	102.86	96.114
$\mathbf{11}_{final}$	8.9746	9.3413	9.4160	95.423	103.17	95.660
$\mathbf{17}_{final}$	9.0784	9.4043	9.4685	94.778	102.24	95.655

Positions

	Tuel et al.[20]			calculated ($\mathbf{0}_{final}$)			atomic displacement
	x	*y*	*z*	*x*	*y*	*z*	(Å)
Al1	0.3006	0.0898	0.8794	0.2798	0.0789	0.8955	0.2206
Al2	0.9025	0.3295	0.0992	0.8751	0.3205	0.0896	0.1393
Al3	0.1740	0.8690	0.3770	0.1530	0.8565	0.3678	0.0899
Al4	0.6850	0.8813	0.0800	0.6584	0.8581	0.0773	0.1813
Al5	0.1054	0.6673	0.8917	0.0891	0.6510	0.8896	0.0822
Al6	0.8342	0.1317	0.6174	0.8128	0.1161	0.6100	0.1004
P7	0.3591	0.8857	0.1227	0.3459	0.8598	0.1176	0.1614
P8	0.1044	0.3331	0.8781	0.0778	0.3231	0.8602	0.1665
P9	0.9479	0.1040	0.3142	0.9082	0.0789	0.3046	0.2709
P10	0.6508	0.1237	0.8735	0.6264	0.1122	0.8705	0.1155
P11	0.9227	0.6546	0.1326	0.9097	0.6436	0.1315	0.0339
P12	0.0455	0.8806	0.6532	0.0355	0.8745	0.6597	0.0901
O13	0.1986	0.9796	0.7196	0.1858	0.9689	0.7357	0.1896
O14	0.2623	0.7581	0.0185	0.2494	0.7435	0.0028	0.1242
O15	0.9879	0.2468	0.7511	0.9628	0.2428	0.7343	0.1659
O16	0.7262	0.2588	0.9778	0.7020	0.2526	0.9710	0.1141
O17	0.8008	0.0077	0.2246	0.7510	0.9943	0.2358	0.3985
O18	0.0508	0.7200	0.2602	0.0489	0.7007	0.2463	0.1820
O19	0.3516	0.0451	0.0209	0.3646	0.0018	0.0503	0.2529
O20	0.2507	0.2659	0.8925	0.2282	0.2559	0.8905	0.1006
O21	0.0581	0.3354	0.0203	0.0211	0.3344	0.9998	0.2667
O22	0.9715	0.2518	0.2591	0.9241	0.2191	0.2317	0.3817
O23	0.0850	0.0230	0.3054	0.0368	0.9953	0.2784	0.3667
O24	0.3098	0.9040	0.2647	0.2859	0.8817	0.2506	0.1676
O25	0.7065	0.9982	0.9534	0.6762	0.9831	0.9492	0.1695
O26	0.7775	0.7270	0.1168	0.7838	0.7350	0.1320	0.2384
O27	0.9721	0.6524	0.9938	0.9418	0.6353	0.9769	0.1894
O28	0.0389	0.7443	0.7319	0.0262	0.7347	0.7342	0.0575
O29	0.9113	0.9634	0.6680	0.8995	0.9514	0.6828	0.1776
O30	0.6992	0.1125	0.7320	0.6801	0.1097	0.7310	0.0950
O31	0.4785	0.1113	0.8410	0.4564	0.1183	0.8397	0.1829
O32	0.5276	0.8636	0.1577	0.5062	0.8142	0.1628	0.4009
O33	0.8743	0.4998	0.1578	0.8532	0.4904	0.1578	0.0958
O34	0.1409	0.4915	0.8493	0.1214	0.4785	0.8241	0.2023
O35	0.0386	0.8371	0.4929	0.0337	0.8390	0.5024	0.1438
O36	0.9419	0.1388	0.4755	0.9157	0.1231	0.4643	0.1394
O37	0.2874	0.7255	0.4878	0.2740	0.7199	0.4725	0.1178
O38	0.3439	0.9846	0.5400	0.2990	0.0025	0.4996	0.5062
O39	0.6599	0.9883	0.4875	0.6516	0.9852	0.4739	0.1237
O40	0.7477	0.3163	0.5524	0.7034	0.2796	0.5385	0.3588
O41	0.0669	0.0175	0.9669	0.0769	0.0209	0.9758	0.2141
O42	0.5483	0.7554	0.9052	0.5533	0.7235	0.9084	0.2829
O43	0.6768	0.7093	0.6253	0.6852	0.7204	0.6703	0.4624
O44	0.0979	0.4750	0.5006	0.1638	0.4494	0.5308	0.7372
O45	0.4760	0.4922	0.0062	0.4976	0.4545	0.9756	0.5265
O46	0.4335	0.5516	0.2877	0.5212	0.6494	0.3928	1.4196
O47	0.4629	0.2409	0.3029	0.5425	0.3797	0.2965	1.5270
O48	0.3446	0.3237	0.5362	0.3796	0.2726	0.4783	0.8458

[a] Space group *P*1 (no. 1).

References and Notes

(1) Wilson, S. T.; Lok, B. M.; Messina, C. A.; Cannan, T. R.; Flanigen, E. M. *J. Am. Chem. Soc.* **1982**, *104*, 1146.

(2) Zanjanchi, M. A.; Rashidi, M. K. *Spectrochim. Acta, Part A* **1999**, *55*, 947.

(3) Flanigen, E. M.; Lok, B. M.; Patton, R. L.; Wilson, S. T. *Stud. Sci. Catal.* **1986**, *28*, 103.

(4) Bennett, J. M.; Dytrych, W. J.; Pluth, J. J.; Richardson, J. W., Jr.; Smith, J. V. *Zeolites* **1986**, *6*, 349.

(5) Oliver, S.; Kuperman, A.; Ozin, G. A. *Angew. Chem., Int. Ed. Engl.* **1998**, *37*, 46.

(6) Flanigen, E. M.; Lok, B. M.; Patton, R. L.; Wilson, S. T. In *Proceedings of the 7th International Zeolite Conference*, Tokyo, 1986; Murakami, Y., Lijima, A., Ward, J. W., Eds.; Elsevier: Amsterdam, 1986; p 103.

(7) Mertens, M.; Martens, J. A.; Grobet, P. J.; Jacobs, P. A. In *Guidelines for mastering the properties of molecular sieves*; Barthomeuf, D., Derouane, E. G., Hölderich, W., Eds.; NATO ASI Series B, Physics, Vol. 221; Plenum Press: New York, 1990; p 1.

(8) D'Arbonneau, S.; Tuel, A.; Auroux A. *J. Therm. Anal. Calorim.* **1999**, *56*, 287.

(9) Blackwell, C. S.; Patton, R. L. *J. Phys. Chem.* **1984**, *88*, 6135.

(10) Kustanovich, I.; Goldfarb, D. *J. Phys. Chem.* **1991**, *95*, 8818.

(11) Prasa, S.; Balakrisknan, I.; Vetrive, R. *J. Phys. Chem.* **1992**, *96*, 3096.

(12) Khouzami, R.; Coudurier, G.; Lefebvre, F.; Vedrine, J. C.; Mentzen, B. F. *Zeolites* **1990**, *10*, 183.

(13) Peeters, M. P. J.; De Hann, J. W.; Van de Ven, L. J. M.; Van Hoof, J. H. C. *J. Phys. Chem.* **1993**, *97*, 5363.

(14) Peeters, M. P. J.; Van de Ven, L. J. M.; De Hann, J. W.; Van Hoof, J. H. C. *J. Phys. Chem.* **1993**, *97*, 8254.

(15) Hartmann, M.; Prakash, A. M.; Kevan, L. *J. Chem. Soc., Faraday Trans.* **1998**, *94* (5), 723−727.

(16) Goepper, M.; Guth, F.; Delmotte, L.; Guth, J. L.; Kessler, H. In *Zeolites: Fact, Figures, Future, Studies in surface science and catalysis*; Jacobs, P. A., Van Santen, R. A., Eds.; Elsevier: Amsterdam, 1989; Vol. 49, p 857.

(17) Bodart, P. R.; Amoureux, J.-P.; Pruski, M.; Bailly, A.; Fernandez, C. *Magn. Reson. Chem.* **1999**, *37*, 569.

(18) Newalkar, B. L.; Jasraa, R. V.; Kamath, V.; Bhat, S. G. T. *Microporous Mesoporous Mater.* **1998**, *20*, 129.

(19) Caldarelli, S.; Meden, A.; Tuel, A. *J. Phys. Chem. B* **1999**, *103*, 5477.

(20) Tuel, A.; Caldarelli, S.; Meden, A.; McCusker, L. B.; Baerlocher, C.; Ristic, A.; Rajic, N.; Mali, G.; Kaucic, V. *J. Phys. Chem. B* **2000**, *104*, 5705.

(21) Van Beest, B. W. H.; Kramer, G. J.; Van Santen, R. A. *Phys. Rev. Lett.* **1990**, *64*, 1955.

(22) De Vos Burchart, E.; Van Bekkum, H.; Van de Graaf, B. *J. Chem. Soc., Faraday Trans.* **1992**, *88*, 2761.

(23) Sastre, G.; Lewis, D. W.; Catlow, C. R. A. *J. Phys. Chem. B* **1997**, *101*, 5249.

(24) Termath, V.; Haase, F.; Sauer, J.; Hutter, J.; Parrinello, M. *J. Am. Chem. Soc.* **1998**, *120*, 8512.

(25) Knops-Gerrits, P.-P.; Toufar, H.; Li, X.-Y.; Grobet, P.; Schoonheydt, R. A.; Jacobs, P. A.; Goddard, W. A. *J. Phys. Chem. A* **2000**, *104*, 2410.

(26) Shott-Darie, C.; Kessler, H.; Benazzi, E. In *Proceedings of the International Symposium on Zeolite Microporous Crystals*, Nagoyan, Japan, 1993; Hattori T., Yashima T., Eds.; Elsevier: Amsterdam, 1994; p 3.

(27) Kessler, H. In *Synthesis, Characterization and Novel Applications of Molecular Sieves Materials*; Bedard, R. L. et al., Eds; Materials Research Society Symposium Proceedings, Vol. 233; Materials Research Society: Pittsburgh, PA, 1991; p 47.

(28) Harding, M. M.; Kariuki, B. M. *Acta Crystallogr. C* **1994**, *50*, 852.

(29) Kessler, H.; Patarin, J.; Schott-Darie, C. *Stud. Surf. Sci. Catal.* **1994**, *85* (Advanced Zeolite Science and Application), 75.

(30) Simmen, A. Ph.D. Thesis, University of Zurich, ETH No. 9710, Switzerland, 1992.

(31) Kresse, G.; Hafner, J. *Phys. Rev. B* **1993**, *47*, 5858.

(32) Kresse, G.; Hafner, J. *Phys. Rev. B* **1993**, *48*, 13115.

(33) Kresse, G.; Hafner, J. *Phys. Rev. B* **1994**, *49*, 14251.

(34) Kresse, G.; Furthmüller, J. *Comput. Mater. Sci.* **1996**, *6*, 15.

(35) Kresse, G.; Furthmüller, J. *Phys. Rev. B* **1996**, *54*, 11169.

(36) Perdew, J. P.; Zunger, A. *Phys. Rev. B* **1981**, *23*, 5048.

(37) Perdew, J. P. In *Electronic Structure of Solids '91*; Ziesche, P., Eschrig, H., Eds.; Akademic verlag: Berlin, 1991; p 11.

(38) Perdew, J. P.; Burke, K.; Wang, Y. *Phys. Rev. B* **1996**, *54*, 16533.

(39) Vanderbilt, D. *Phys. Rev. B* **1990**, *41*, 7892.

(40) Kresse, G.; Hafner, J. *J. Phys. Condens. Matter* **1994**, *6*, 8245.

(41) Payne, M. C.; Teter, M. P.; Allan, D. C.; Arias, T. A.; Joannopoulos, J. D. *Rev. Mod. Phys.* **1992**, *64*, 1045.

(42) Kresse, G.; Joubert, J. *Phys. Rev. B* **1999**, *59*, 1758.

(43) Blöch, P. E. *Phys. Rev. B* **1994,** *50*, 17953.

(44) Monkhorst, H. J.; Pack, J. D. *Phys. Rev. B* **1976**, *13*, 5188.

(45) Jeanvoine, Y.; Angyán, J. G.; Kresse, G.; Hafner, J. *J. Phys. Chem. B* **1998**, *102*, 5573.

(46) Jeanvoine, Y.; Angyán, J. G.; Kresse, G.; Hafner, J. *J. Phys. Chem. B* **1998**, *102*, 7307.

(47) Barbosa, L. A.; Van Santen, R. A.; Hafner, J. *J. Am. Chem. Soc.* **2001**, *123*, 4530.

(48) Leeuw, N. H.; Purton, J. A.; Parker, S. C.; Watson, G. W.; Kresse, G. *Surf. Sci.* **2000**, *452*, 9.
(49) Nosé, S. *J. Chem. Phys.* **1984**, *81*, 511.
(50) Nosé, S. *Prog. Theor. Phys. Suppl.* **1991**, *103*, 1.
(51) Allen, M. P.; Tidesley, D. J. *Computer Simulations of liquids*; Clarendon: Oxford, U.K., 1987.
(52) Jeffrey, G. A. *An introduction to hydrogen bonding*; Topics in physical chemistry series; Oxford University Press: New York, 1997.
(53) Singh, U. C.; Kollman, P. A. *J. Chem. Phys.* **1985**, *83*, 4033.
(54) Chakravorty, S. J.; Davidson, E. R. *J. Phys. Chem.* **1993**, *97*, 6373.
(55) Hamann, D. R. *Phys. Rev. B* **1997**, *55*, R10157.
(56) Sirois, S.; Proynov, E. I.; Nguyen, D. T.; Salahub, D. R. *J. Chem. Phys* **1997**, *107*, 6770.
(57) Turki, N.; Milet, A.; Ouamerali, O.; Moszynski, R.; Kochanski, E. *J. Mol. Struct. (THEOCHEM)* **2002**, *577*, 239.
(58) Vassilev, P.; Hartnig, C.; Koper, M. T. M.; Frechard, F.; van Santen, R. A *J. Chem. Phys.* **2001**, *115*, 9815.
(59) Tsuzuki, S.; Luthi, H. P. *J. Chem. Phys.* **2001**, *114*, 3949.
(60) Boudias, C.; Monceau, D. *CaRIne Crystallography*, version 3-1; Divergent S.A.: Compiegne, France, 1998.
(61) Kaszkur, Z. A.; Jones, R. H.; Waller, D.; Catlow, C.; Richard, A.; Thomas, J. M. *J. Phys. Chem.* **1993**, *97*, 426.